

MATHEMATICS OF LINEAR SWEEPS

DAVID F. ALDRIDGE¹

ABSTRACT

The linear sweep is the most common swept frequency signal used in seismic exploration. Despite this fact, there exists a plethora of erroneous or ambiguous formulae in the published literature for the autocorrelation function and the Fourier spectrum of the linear sweep. *Mathematically exact expressions for each are derived here.* These serve to correct many of the existing equations, and hence have educational value. Moreover, the exact formulae allow numerical modelling experiments with linear sweeps and/or Klauder wavelets to be carried out with speed and high accuracy.

INTRODUCTION

In the geophysical literature, there is a long history of erroneous formulae relating to swept frequency signals. These expressions can serve as an impediment to education and research on this topic. The errors and ambiguities need not be dwelt upon here, but range from prosaic (sign errors) to perplexing (autocorrelation wavelets that lack even symmetry; Fourier spectra that lack Hermitian symmetry). Additionally, some approximate formulae are presented as if they are exact expressions, thereby creating more needless puzzlement. The existing situation motivates the presentation of this tutorial on the basic mathematics of swept frequency signals.

The primary purpose of this paper is to derive exact mathematical expressions for the autocorrelation function and the Fourier spectrum of the linear sweep. These exact formulae are useful for theoretical work, computational modelling and educational purposes. They also allow an objective evaluation of various published (or proposed) approximations for the autocorrelation wavelet and Fourier transform. The derived formulae are equally applicable to upsweeps or downsweeps.

A strictly mathematical viewpoint is adopted. Practical issues related to the generation and reception of swept frequency signals in any particular experimental context are not discussed. However, in order to illustrate the utility of the derived equations, a simple application to extended correlation of industry Vibroseis data is described.

DEFINITIONS

A general mathematical definition of a swept frequency signal is

$$s(t) = a(t) \cos \theta(t), \quad (1)$$

where $a(t)$ is the *amplitude function* and $\theta(t)$ is the *phase function*. The *frequency function* is defined by

$$f(t) = \frac{1}{2\pi} \frac{d\theta(t)}{dt}. \quad (2)$$

Hence, the frequency function can be determined by differentiation if the phase function is specified. Alternately, the phase function can be derived from a given frequency function by integration:

$$\theta(t) = \theta_0 + 2\pi \int_0^t f(\tau) d\tau, \quad (3)$$

where θ_0 is a constant phase angle.

Note that $a(t)$, $\theta(t)$ and $f(t)$ are not referred to as the *instantaneous* amplitude, phase and frequency, respectively. The instantaneous attributes of a real function $s(t)$ are defined in terms of its complex-valued analytic signal $s(t) - i\hat{s}(t)$, where $\hat{s}(t)$ is the Hilbert transform of $s(t)$ (Bracewell, 1965, p. 267-272). For a swept frequency signal, these attributes are not necessarily equal to the amplitude, phase and frequency functions given above. The derivation of exact mathematical formulae for the instantaneous attributes of a swept frequency function requires additional research, and is not pursued further in this paper.

In the sequel, frequent use is made of the standard functions $\Pi(x)$, $\Lambda(x)$, $\text{sgn}(x)$ and $\text{sinc}(x)$ (Bracewell, 1965, p. 67). $\Pi(x)$ and $\Lambda(x)$ are the rectangle and triangle functions of unit height and area, respectively [$\Pi(x) = 1$ for $|x| \leq 1/2$, zero otherwise; $\Lambda(x) = 1 - |x|$ for $|x| \leq 1$, zero otherwise]. The signum function is defined by $\text{sgn}(x) = x/|x|$ for nonzero x and $\text{sgn}(0) = 0$. Finally, $\text{sinc}(x) = \sin(\pi x)/\pi x$.

UNTAPERED LINEAR SWEEP

The amplitude function that is most amenable to mathematical analysis is a rectangle function with constant height

Manuscript received by the Editor September 23, 1991; revised manuscript received December 28, 1991.

¹University of British Columbia, Department of Geophysics and Astronomy, 129 - 2219 Main Mall, Vancouver, British Columbia V6T 1Z4

Support for this research was provided by Natural Sciences and Engineering Research Council (NSERC) operating grant 5-84270 (principal investigator: Professor D.W. Oldenburg) and a Killam Predoctoral Fellowship from the University of British Columbia.

A and base width equal to the sweep duration T . There is no loss in generality in assuming the onset time of the sweep to be $t_0 = 0$. Hence,

$$a(t) = A\pi \left[\frac{t}{T} - \frac{1}{2} \right]. \quad (4)$$

The step discontinuities in this amplitude function at $t = 0$ and $t = T$ introduce undesirable oscillations into the autocorrelation function and the Fourier transform of the sweep. Hence, some form of short duration tapering is usually applied at each end of $a(t)$. A common amplitude taper called the *cosine taper* is analysed in a subsequent section. A sweep with the amplitude function (4) is referred to as an *untapered sweep*.

The form of the frequency function has a strong influence on the Fourier spectrum of a swept frequency signal. Goupillaud (1976) illustrates the spectral shaping effects produced by various monotonic frequency functions. The simplest of these is the linear frequency function given by

$$f(t) = f_1 + \left[\frac{f_2 - f_1}{T} \right] t, \quad 0 \leq t \leq T \quad (5)$$

where f_1 is the *start frequency* and f_2 is the *end frequency*. $f(t)$ is taken to be zero outside the time interval $[0, T]$. Other quantitative descriptors of the linear frequency function are the *sweep rate* $r \equiv (f_2 - f_1)/T$, the *bandwidth* $W \equiv |f_2 - f_1|$ and the *centre frequency* $f_c \equiv (f_1 + f_2)/2$. The sweep rate can be positive or negative, corresponding to an *upsweep* ($f_2 > f_1$) or a *downsweep* ($f_2 < f_1$), respectively. However, the bandwidth and centre frequency are strictly nonnegative.

Substituting (5) into (3) and integrating yields an expression for the phase function of the linear sweep:

$$\begin{aligned} \theta_0, & \quad t < 0 \\ \theta(t) = \theta_0 + 2\pi \left(f_1 + \frac{rt}{2} \right) t, & \quad 0 \leq t \leq T \\ \theta_0 + 2\pi \left(f_1 + \frac{rT}{2} \right) T, & \quad T < t \end{aligned} \quad (6)$$

Thus, the phase is a quadratic function of time within the basic interval $0 \leq t \leq T$. Finally, combining the amplitude function (4) and the phase function (6) in the general expression (1) gives a compact formula for the untapered linear sweep:

$$s(t) = A \cos(\theta_0 + 2\pi f_1 t + \pi r t^2), \quad 0 \leq t \leq T \quad (7)$$

with $s(t) = 0$ for $t < 0$ or $t > T$.

The inclusion of an adjustable initial phase angle θ_0 in (7) allows greater flexibility in the generation of linear sweep signals. In the particular case where $\theta_0 = -\pi/2$, equation (7) reduces to analogous sweep formulae given by Serif and Kim (1970), Goupillaud (1976), Waters (1978, p. 81) and Cunningham (1979). In contrast, Klauder et al. (1960), Geyer (1970), Carroll (1971) and Gurbutz (1972) implicitly adopt the value $\theta_0 = -\pi(3f_1 + f_2)T/4$ for the initial phase. This choice forces the phase function $\theta(t)$ to equal zero at the half duration time. In their developments, the initial phase angle is not considered a free parameter in the definition of a sweep. Rather, it is determined by the remaining parameters f_1, f_2

and T . Finally, Rietsch (1977a, b) and Kanasewich (1981, p. 91; 1990, p. 199) include an independent initial phase angle in their sweep expressions.

AUTOCORRELATION FUNCTION

The autocorrelation function of a real signal $s(t)$ is defined as

$$\phi_{ss}(t) = \int_{-\infty}^{+\infty} s(\tau) s(\tau - t) d\tau. \quad (8)$$

Substituting (7) into (8) and integrating yields the following expression for the autocorrelation function of the untapered linear sweep:

$$\begin{aligned} \phi_{ss}(t) = & \frac{A^2 T}{2} \left\{ \Lambda(t/T) \operatorname{sinc} [Wt(1 - |t|/T)] \cos(2\pi f_c t) \right. \\ & + \frac{1}{2\sqrt{WT}} \cos \alpha(t) [C(u_2(t)) - C(u_1(t))] \\ & \left. + \frac{1}{2\sqrt{WT}} \sin \alpha(t) [S(u_2(t)) - S(u_1(t))] \right\}. \quad (9) \end{aligned}$$

In this expression, $C(x)$ and $S(x)$ are the real and imaginary parts of the complex Fresnel integral

$$F(x) = C(x) + iS(x) = \int_0^x \exp(i\frac{\pi}{2} u^2) du. \quad (10)$$

Hence,

$$C(x) = \int_0^x \cos(\frac{\pi}{2} u^2) du, \quad (11a)$$

$$S(x) = \int_0^x \sin(\frac{\pi}{2} u^2) du. \quad (11b)$$

Spanier and Oldham (1987, p. 373-383) describe many of the salient characteristics of the Fresnel cosine and sine integrals. They also provide a simple algorithm for accurate numerical evaluation of the related quantities $C(\sqrt{2/\pi} x)$ and $S(\sqrt{2/\pi} x)$. The arguments of the Fresnel integrals in (9) are functions of time defined by

$$u_1(t) = \sqrt{WT} \left[\frac{2f_c}{W} - \Lambda(t/T) \right], \quad (12a)$$

$$u_2(t) = \sqrt{WT} \left[\frac{2f_c}{W} + \Lambda(t/T) \right]. \quad (12b)$$

Figure 1 depicts these two functions; note that if $|t| \geq T$, then $u_1(t)$ and $u_2(t)$ both equal $2f_c \sqrt{T/W}$. Finally, the angle $\alpha(t)$ in equation (9) is a quadratic function of time given by

$$\alpha(t) = \operatorname{sgn}(r) \left\{ 2\pi r T^2 \left[\left(\frac{f_1}{W} \right)^2 - \left(\frac{t}{2T} \right)^2 \right] - 2\theta_0 \right\}. \quad (13)$$

Formula (9) for $\phi_{ss}(t)$ satisfies the obvious requirements for an autocorrelation function of a finite duration signal: it is dimensionally correct, it is even in t , and it vanishes for $|t| \geq T$. Moreover, the expression is valid for either an upsweep

($r > 0$) or a downsweep ($r < 0$). Many existing autocorrelation formulae contain the factor \sqrt{r} (or $\sqrt{f_2 - f_1}$) (Gurbuz, 1972; Cunningham, 1979; Kanasewich, 1981, p. 92; 1990, p. 201). These expressions can be applied to a downsweep only by generalizing the Fresnel integrals in (11a, b) above to include complex-valued arguments. The fact that an upsweep and a downsweep with the same centre frequency, bandwidth and duration may yield different autocorrelation functions is evident upon rewriting the angle $\alpha(t)$ in (13) as follows:

$$\alpha(t) = 2\pi WT \left[\left(\frac{f_c}{W} \right)^2 + \frac{1}{4} - \left(\frac{t}{2T} \right)^2 \right] - \text{sgn}(r) [2\pi f_c T + 2\theta_0]. \quad (14)$$

Dependence on the sweep rate r is contained entirely in the second term on the right hand side. Substituting (14) into (9) reveals that the autocorrelation of the upsweep and downsweep are identical only if $2\pi f_c T + 2\theta_0 = n\pi$, where n is an integer. In terms of the sweep itself [equation (7)], this condition implies that $s(T) = (-1)^n s(0)$, i.e., the value of the sweep at the end time T equals, to within a sign factor, its value at the start time.

Geyer (1970) refers to the autocorrelation function $\phi_{ss}(t)$ as a Klauder wavelet, although his expression omits the terms involving the Fresnel integrals. These terms contribute low amplitude oscillations to the autocorrelation that are most evident at large absolute times. Neglecting the terms containing the Fresnel integrals yields an approximate sweep autocorrelation given by

$$\tilde{\phi}_{ss}(t) = \frac{A^2 T}{2} \Lambda(t/T) \text{sinc}[Wt(1 - |t|/T)] \cos(2\pi f_c t). \quad (15)$$

$$S_u(f) = \frac{A}{2} \sqrt{\frac{T}{2W}} \left\{ e^{+i\theta_0} [F(v_2(f)) - F(v_1(f))] \exp\left(-i\frac{\pi}{2} v_1(f)^2\right) + e^{-i\theta_0} [F(w_2(f)) - F(w_1(f))]^* \exp\left(+i\frac{\pi}{2} w_1(f)^2\right) \right\}, \quad (18a)$$

$$S_d(f) = \frac{A}{2} \sqrt{\frac{T}{2W}} \left\{ e^{+i\theta_0} [F(v_1(f)) - F(v_2(f))]^* \exp\left(+i\frac{\pi}{2} v_1(f)^2\right) + e^{-i\theta_0} [F(w_1(f)) - F(w_2(f))] \exp\left(-i\frac{\pi}{2} w_1(f)^2\right) \right\}, \quad (18b)$$

Interestingly, this approximation retains all of the desirable properties of the exact autocorrelation $\phi_{ss}(t)$ that are mentioned above. Moreover, it is independent of the sign of the sweep rate and the value of the initial phase angle. A final approximation is obtained by assuming $|t|/T \ll 1$ in (15):

$$\tilde{\phi}_{ss}(t) = \frac{A^2 T}{2} \text{sinc}(Wt) \cos(2\pi f_c t). \quad (16)$$

This form is instructive because it yields a very simple expression for the energy density spectrum (or power spec-

trum) of the linear sweep: two rectangles of height $A^2 T/4W$, width W , and centred at $\pm f_c$. Cunningham (1979) attempts a similar short time approximation for the Klauder wavelet, but obtains an expression that is not even in t and is sensitive to the sign of the sweep rate.

Figure 2a displays the central portion of a Klauder wavelet defined by the parameter values $f_1 = 10$ Hz, $f_2 = 80$ Hz, $T = 12$ s, $\theta_0 = -\pi/2$ radians and $A = 1$. The wavelet is calculated from the exact autocorrelation formula (9). Over the displayed time window, the exact wavelet is almost indistin-

guishable from the approximations given in (15) and (16) at this plot scale. The difference between expressions (9) and (15) at large time lags is illustrated in Figure 2b. These low amplitude oscillations comprise part of the 'correlation noise' background of a correlated seismic trace.

FOURIER TRANSFORM

The Fourier transform of the signal $s(t)$ is defined as

$$S(f) = \int_{-\infty}^{+\infty} s(t) e^{-i2\pi ft} dt. \quad (17)$$

Expressions for the Fourier transform of the untapered linear sweep are obtained by substituting (7) into (17) and integrating. The upsweep and downsweep cases are treated separately. The results are

where the subscripts u and d refer to the upsweep and downsweep, respectively. The arguments of the complex Fresnel integrals in (18a, b) are linear functions of frequency given by

$$v_1(f) = \sqrt{\frac{2T}{W}} (f_1 - f), \quad v_2(f) = \sqrt{\frac{2T}{W}} (f_2 - f), \quad (19a, b)$$

$$w_1(f) = \sqrt{\frac{2T}{W}} (f_1 + f), \quad w_2(f) = \sqrt{\frac{2T}{W}} (f_2 + f). \quad (19c, d)$$

Thus, $v_1(f)$ and $v_2(f)$ decrease monotonically with frequency while $w_1(f)$ and $w_2(f)$ are monotonically increasing. Since $v_1(-f) = w_1(f)$ and $v_2(-f) = w_2(f)$, equations (18a, b) possess the Hermitian symmetry required for the Fourier transform of a real signal: $S_u(-f) = S_u(f)^*$ and likewise for $S_d(f)$. Expressions for the Fourier transform of an untapered linear sweep given by Klauder et al. (1960), Gurbuz (1972), Goupillaud (1976) and Kanasewich (1981, p. 93; 1990, p. 202) are not Hermitian and thus cannot be the transform of a real signal $s(t)$. An approximate representation of the sweep spectrum is derived by Rietsch (1977a) by evaluating the Fourier transform integral (17) via the method of stationary phase.

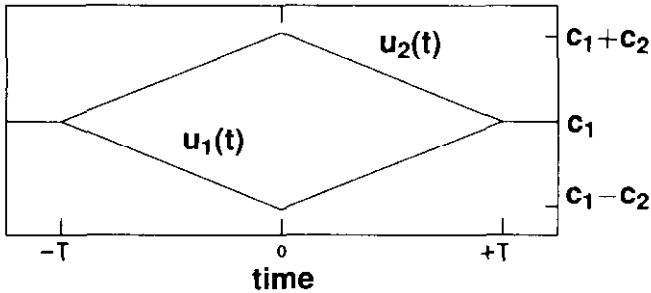


Fig. 1. Graph of the arguments $u_1(t)$ and $u_2(t)$ to the Fresnel integrals. Constants c_1 and c_2 are $c_1 = 2f_c \sqrt{T/W}$ and $c_2 = \sqrt{WT}$.

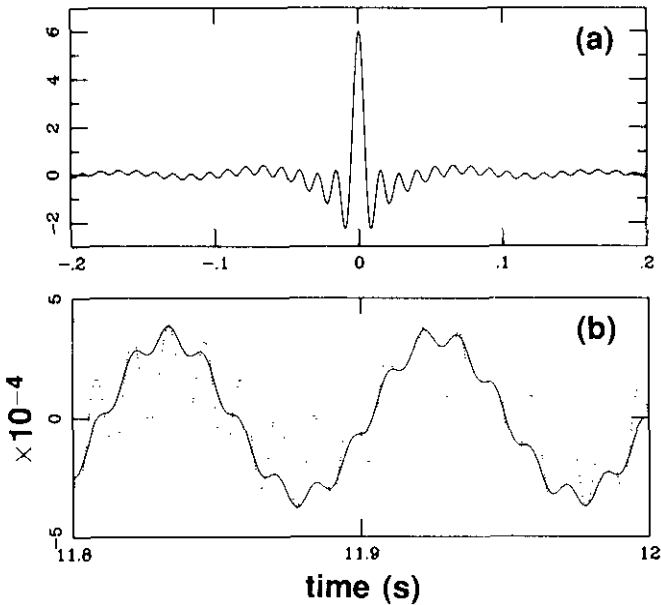


Fig. 2. (a) Central portion of a broadband Klauder wavelet calculated via the exact autocorrelation formula. (b) Comparison of exact (solid curve) and approximate (dotted curve) expressions for the same Klauder wavelet at large time lags. The zero time value of the wavelet is normalized to unity in (b).

Amplitude, phase and energy density spectra calculated from formula (18a) are depicted in Figure 3. Sweep parameter values are identical to those used in Figure 2. The rectangular spectra plotted in panels (a) and (c) correspond to the Fourier transform of the approximation (16):

$$\bar{\Phi}_{ss}(f) = \frac{A^2 T}{4W} \left\{ \Pi \left[\frac{f-f_c}{W} \right] + \Pi \left[\frac{f+f_c}{W} \right] \right\}. \quad (20)$$

Rietsch's (1977a) approximation to the amplitude spectrum is identical to $\sqrt{\bar{\Phi}_{ss}(f)}$. Strong oscillations are clearly evident on the amplitude spectrum plot in Figure 3a. These are magnified, relative to the ideal (rectangular) spectrum, on the plot of the energy density spectrum. Numerous published graphs of energy density spectra do not reveal this fine structure (e.g., Kanasewich, 1981, p. 94; 1990, p. 203) and thus are probably sampled too grossly to detect it. The frequency sampling interval used for Figure 3 is 0.04 Hz, corresponding to 2501 samples from 0 to 100 Hz.

The phase spectrum displayed in Figure 3b is unwrapped using Schafer's algorithm (Oppenheim and Schafer, 1975, p. 508-509). The small frequency sampling interval allows this simple phase unwrapping method to operate successfully. The shape of the unwrapped curve is approximately parabolic, as noted previously by Rietsch (1977a) and Poggiagliolmi et al. (1982). Rietsch's parabolic approximation to the true phase spectrum is $\theta_0 \pm (\pi/4) \mp (\pi/2)v_1(f)^2$ (upper signs for an upsweep and lower signs for a downsweep) and is plotted as the lower curve in Figure 3b. For this example, it is an excellent approximation over the nominal frequency band (within $\pm 5^\circ$ from 15 to 75 Hz).

COSINE-TAPERED LINEAR SWEEP

Many authors emphasize the benefits of tapering the ends of the amplitude function $a(t)$ (e.g., Edelmann, 1966; Gurbuz, 1972; Goupillaud, 1976). Gradual tapering reduces the magnitude of the oscillations introduced into the autocorrelation function and the amplitude spectrum of the sweep. In this section, the common cosine taper is briefly analysed.

Let T_1 and T_2 be the lengths of the taper zones at the start and end of the sweep. Then, the amplitude function of the cosine-tapered sweep is

$$a(t) = \begin{cases} 0, & t < 0 \\ (A/2) \left[1 - \cos\left(\frac{\pi t}{T_1}\right) \right], & 0 \leq t \leq T_1 \\ A, & T_1 < t < T - T_2 \\ (A/2) \left[1 + \cos\left(\frac{\pi(t - T + T_2)}{T_2}\right) \right], & T - T_2 \leq t \leq T \\ 0, & T < t \end{cases} \quad (21)$$

This tapering makes the derivative $a'(t)$ continuous. Hence, the amplitude function (21) is considerably smoother than the previous function (4). Expression (21) may be rewritten as

$$a(t) = A\Pi\left[\frac{t}{T} - \frac{1}{2}\right] - A\Pi\left[\frac{t}{T_1} - \frac{1}{2}\right] \cos^2\left(\frac{\pi t}{2T_1}\right) - A\Pi\left[\frac{t-T}{T_2} + \frac{1}{2}\right] \sin^2\left(\frac{\pi(t-T+T_2)}{2T_2}\right). \quad (22)$$

The first term on the right hand side of (22) is the amplitude function of an untapered sweep. The remaining two terms represent correction factors that account for the cosine tapers at each end of the sweep.

Multiplying $a(t)$ in (22) by $\cos \theta(t)$ [where $\theta(t)$ is the quadratic phase function (6)] yields a three term expression for the cosine-tapered linear sweep. It is possible to evaluate the Fourier transform integral (17) for each term of this sweep; a set of expressions similar to equations (18a, b) are obtained. Since these formulae are lengthy, they are stated in the Appendix. The result is a closed form mathematical expression for the spectrum of a cosine-tapered sweep that is quite useful for modelling purposes (e.g., Aldridge, 1989). Figure 4 illustrates amplitude and energy density spectra calculated via this formula. The severe oscillations visible on the previous spectra are now almost completely damped out except for small overshoots near each sweep terminal frequency. However, as indicated, the tapering does result in a reduction of spectral bandwidth.

APPLICATION TO EXTENDED VIBROSEIS CORRELATION

Extended correlation of Vibroseis data is a method of extracting deep crust and Moho reflections from a data set originally recorded for shallow exploration objectives (Okaya and Jarchow, 1989; Zelt and Ellis, 1989). Conventional correlation of the seismic data typically yields only a restricted set of positive time lags for the output traces. In particular, if the field record length is t_{record} , then the correlated record length is commonly $t_{record} - T$, where T is the sweep duration. Within this time interval, the maximum spectral bandwidth of reflection wavelets is constant and approximately equal to the bandwidth W of the sweep frequency function. However, if the correlation process is continued to greater positive time lags, deeper reflections may be observed, albeit with reduced bandwidth. In many cases this loss of bandwidth is acceptable because only the low-frequency energy penetrates to great depths and is returned. Also, much interpretation of deep crust and Moho reflections requires only the detection of the signal, rather than detailed waveform analysis.

Okaya and Jarchow (1989) describe the extended correlation process in terms of time-domain correlation operations. However, if the correlated trace is actually generated by frequency-domain manipulations, then correlated output at all time lags (including the negative lags) is automatically created. Extended correlation processing then reduces to the

trivial task of making the full set of output time lags available for further processing, analysis or interpretation.

The above equations can be used to estimate the maximum bandwidth of reflection wavelets expected in extended correlation data. Let $s(t; T_s)$ denote the sweep generated by the Vibroseis energy source, where T_s is the source sweep duration. A recorded sweep $s(t; T_r)$ has a duration T_r , that is less than or equal to T_s . Specifically, if the two-way travel-time t_r of a reflection impulse is greater than $t_{record} - T_s$, then the reflected sweep is truncated by the finite length recording window to duration $T_r = t_{record} - t_r$. Finally, the sweep signal used for correlation of the field traces is designated $s(t; T_c)$. Typically $T_c = T_s$, i.e., the source sweep is used as the correlation operator. If $T_c < T_s$, then a uniform, but diminished, reflection bandwidth is maintained over a longer time interval on the output record (Okaya and Jarchow, 1989).

The wavelet associated with a reflection impulse is obtained by crosscorrelating the recorded sweep with the correlation operator:

$$\phi_{rc}(t) = \int_{-\infty}^{+\infty} s(\tau; T_r) s(\tau - t; T_c) d\tau. \quad (23)$$

Note that if $T_r = T_c = T_s$, then (23) reduces to the prior expression (8) for the autocorrelation of the source sweep. The Fourier transform of $\phi_{rc}(t)$ is the cross-spectrum

$$\Phi_{rc}(f) = S(f; T_r) S(f; T_c)^*. \quad (24)$$

Figure 5 plots the amplitudes of six cross-spectra for the case where $T_c = T_s = 12$ s, and $T_r = 12, 10, 8, 6, 4$ and 2 s. If the total record length is $t_{record} = 16$ s, then these recorded sweep durations correspond to reflection impulses with two-way traveltimes of $t_r = 4, 6, 8, 10, 12$ and 14 s. All of these upsweeps have the same start frequency $f_1 = 10$ Hz, rate $r = 5.833$ Hz/s, initial phase angle $\theta_0 = -\pi/2$ radians, amplitude $A = 1$ and 0.5 s cosine taper. However, the end frequencies of the recorded sweeps are progressively reduced from 80 Hz, to $68.33, 56.67, 45.00, 33.33$ and 21.67 Hz, respectively. The corresponding narrowing of the amplitude spectra is evident in the figure.

Finally, the parabolic approximation to the sweep phase spectrum (Rietsch, 1977a) is used to estimate phase spectra associated with each of the above cross-spectra. Since all sweeps have the same start frequency, rate and initial phase angle, the approximation implies that each phase spectrum equals zero over the nominal passband. This is confirmed by digitally unwrapping the phase spectra computed from equation (24) above.

CONCLUSION

The mathematical analysis presented herein should be of interest to those performing computational modelling experiments with linear sweeps and/or Klauder wavelets. The exact formulae for the autocorrelation function and the Fourier spectrum of a sweep are straightforward to evaluate. Hence, speed and accuracy can be maintained where necessary in numerical

work. Finally, a thorough and rigorous understanding of the linear sweep is a necessary prelude to the analysis of sweeps with more complicated frequency and amplitude modulation.

REFERENCES

Aldridge, D.F., 1989, Statistically perturbed geophone array responses: *Geophysics* **54**, 1306-1317.
 Bracewell, R., 1965, *The Fourier transform and its applications*: McGraw-Hill Book Co.
 Carroll, P., 1971, A note on synthetic Vibroseis sweep generation: *J. Can. Soc. Expl. Geophys.* **7**, 80-81.
 Cunningham, A.B., 1979, Some alternate vibrator signals: *Geophysics* **44**, 1901-1921.
 Edelmann, H., 1966, New filtering methods with Vibroseis: *Geophys. Prosp.* **14**, 455-469.
 Geyer, R.L., 1970, The Vibroseis system of seismic mapping: *J. Can. Soc. Expl. Geophys.* **6**, 39-57.
 Goupillaud, P.L., 1976, Signal design in the Vibroseis technique: *Geophysics* **41**, 1291-1304.
 Gurbuz, B.M., 1972, Signal enhancement of vibratory source data in the presence of attenuation: *Geophys. Prosp.* **20**, 421-438.
 Kanasewich, E.R., 1981, *Time sequence analysis in geophysics*: Univ. of Alberta Press.
 _____. 1990, *Seismic noise attenuation*: Pergamon Press, Inc.

Klauder, J.R., Price, A.C., Darlington, S. and Albersheim, W.J., 1960, The theory and design of chirp radars: *Bell System Tech. J.* **39**, 745-808.
 Okaya, D.A. and Jarchow, C.M., 1989, Extraction of deep crustal reflections from shallow Vibroseis data using extended correlation: *Geophysics* **54**, 555-562.
 Oppenheim, A.V. and Schaffer, R.W., 1975, *Digital signal processing*: Prentice-Hall, Inc.
 Poggiagliolmi, E., Berkhout, A.J. and Boone, M.M., 1982, Phase unwrapping, possibilities and limitations: *Geophys. Prosp.* **30**, 281-291.
 Rietsch, E., 1977a, Computerized analysis of Vibroseis signal similarity: *Geophys. Prosp.* **25**, 541-552.
 _____. 1977b, Vibroseis signals with prescribed power spectrum: *Geophys. Prosp.* **25**, 613-620.
 Serif, A.J. and Kim, W.H., 1970, The effect of harmonic distortion in the use of vibratory surface sources: *Geophysics* **35**, 234-246.
 Spanier, J. and Oldham, K.B., 1987, *An atlas of functions*: Hemisphere Publishing Corp.

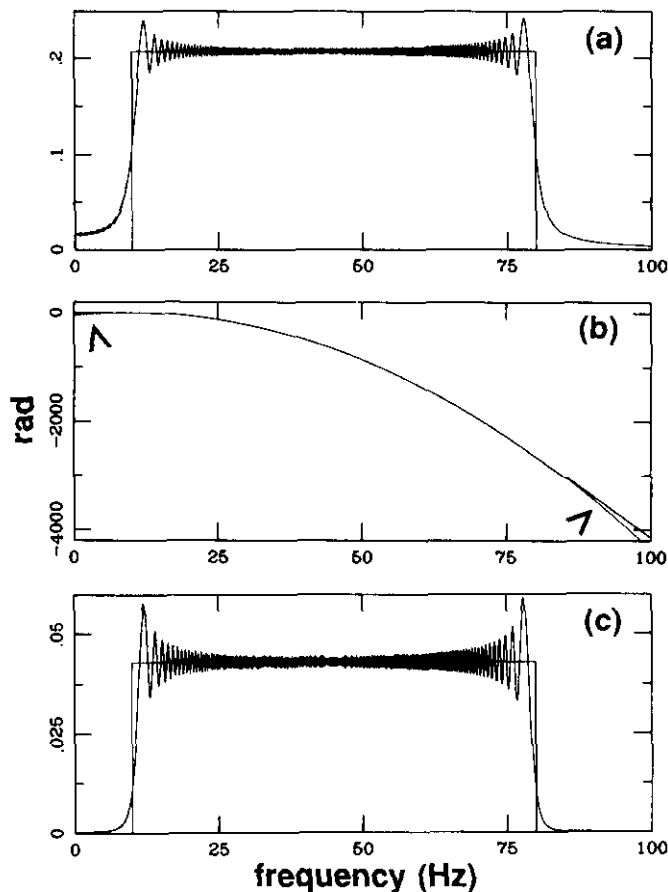


Fig. 3. Amplitude (a), phase (b) and energy density (c) spectra for an untapered linear up-sweep defined by $f_1 = 10$ Hz, $f_2 = 80$ Hz, $T = 12$ s, $\theta_0 = -\pi/2$ radians and $A = 1$. Rectangular spectra in panels (a) and (c) are ideal spectra. Arrows in panel (b) highlight the small difference between exact (upper curve) and approximate (lower curve) phase spectra.

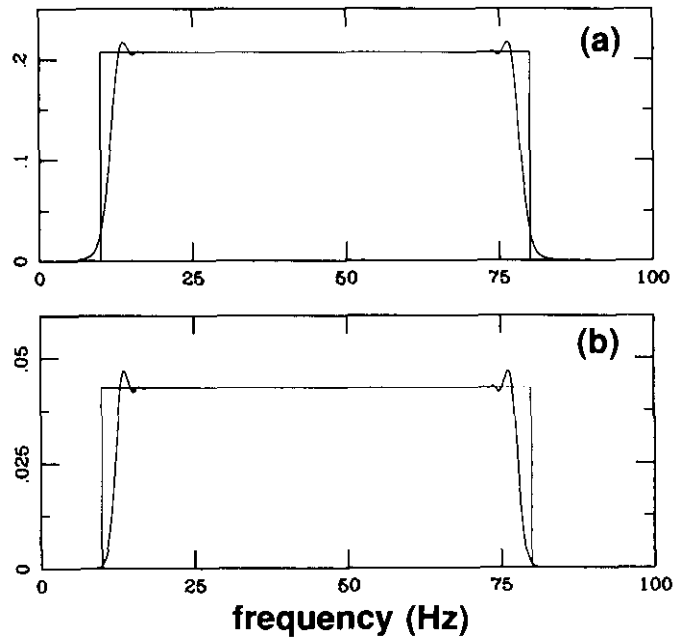


Fig. 4. Amplitude (a) and energy density (b) spectra after application of a 0.5 s cosine taper to each end of the linear up-sweep used for Figure 3. Rectangular spectra are ideal spectra.

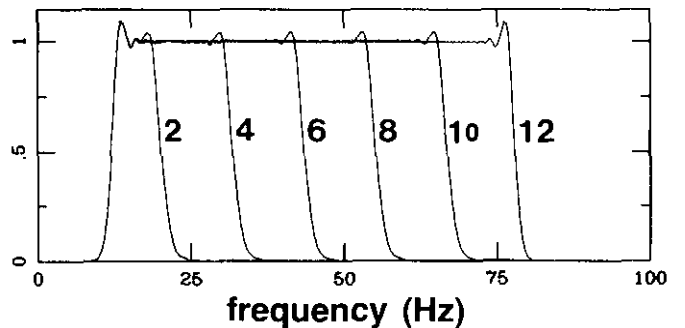


Fig. 5. Amplitudes of six cross spectra obtained by correlating a 12 s source sweep with recorded sweeps having durations of 2, 4, 6, 8, 10 and 12 s. All other up-sweep parameters are identical. The vertical scale is adjusted so that the flat portion common to all spectra plots at 1.0.

Waters, K.H., 1978, Reflection seismology, a tool for energy resource exploration: John Wiley & Sons, Inc.
 Zelt, C.A. and Ellis, R.M., 1989, Comparison of near-coincident crustal refraction and extended Vibroseis reflection data: Peace River region, Canada: Geophys. Res. Lett. **16**, 843-846.

The correction factor associated with the back end cosine taper (from $T - T_2$ to T) is slightly more complicated because it does not begin at zero time. It is

$$S_2(f) = -\frac{A}{4} \sqrt{\frac{T}{2W}} \left\{ e^{+i\theta_0} \left[G(v_2, v_8, v_1) + \frac{1}{2} G(v_{10}, v_9, v_{13}) + \frac{1}{2} G(v_{12}, v_{11}, v_{14}) \right] + e^{-i\theta_0} \left[G(w_2, w_8, w_1) + \frac{1}{2} G(w_{10}, w_9, w_{13}) + \frac{1}{2} G(w_{12}, w_{11}, w_{14}) \right]^* \right\}, \quad (A4)$$

APPENDIX

Expressions for the Fourier transform of the cosine-tapered linear upsweep are given in this Appendix. The appropriate formulae for the downsweep are omitted for brevity. Notation is simplified by defining a complex-valued function G with three real arguments:

$$G(x, y, z) \equiv [F(x) - F(y)] \exp\left(-i\frac{\pi}{2}z^2\right). \quad (A1)$$

In terms of this new function, the Fourier transform of the untapered upsweep [equation (18a)] becomes

$$S_u(f) = \frac{A}{2} \sqrt{\frac{T}{2W}} \left\{ e^{+i\theta_0} G(v_2, v_1, v_1) + e^{-i\theta_0} G(w_2, w_1, w_1)^* \right\}, \quad (A2)$$

where v_1, v_2, w_1 and w_2 represent the linear functions of frequency defined in equations (19).

Equation (A2) corresponds to the first term on the right-hand side of (22) in the text. The Fourier transform of the second term gives a correction factor associated with the front end cosine taper of length T_1 . It is

$$S_1(f) = -\frac{A}{4} \sqrt{\frac{T}{2W}} \left\{ e^{+i\theta_0} \left[G(v_3, v_1, v_1) + \frac{1}{2} G(v_5, v_4, v_4) + \frac{1}{2} G(v_7, v_6, v_6) \right] + e^{-i\theta_0} \left[G(w_3, w_1, w_1) + \frac{1}{2} G(w_5, w_4, w_4) + \frac{1}{2} G(w_7, w_6, w_6) \right]^* \right\}. \quad (A3)$$

The argument $v_3(f)$ is given by

$$v_3(f) = \sqrt{\frac{2T}{W}} (f(T_1) - f),$$

where the value of the frequency function at time T_1 is $f(T_1) = f_1 + (T_1/T)W$. The other arguments are related to $v_1(f)$ and $v_3(f)$ in a simple way. Define a dimensionless frequency shift $\Delta_1 \equiv \sqrt{2T/W}(1/2T_1)$. Then

$$\begin{aligned} v_4(f) &= v_1(f) + \Delta_1, & v_5(f) &= v_3(f) + \Delta_1, \\ v_6(f) &= v_1(f) - \Delta_1, & v_7(f) &= v_3(f) - \Delta_1. \end{aligned}$$

The arguments $w_i(f)$ are all obtained via $w_i(f) = v_i(-f)$.

where the argument $v_8(f)$ is given by

$$v_8(f) = \sqrt{\frac{2T}{W}} (f(T - T_2) - f).$$

The other arguments are related to $v_2(f)$ and $v_8(f)$ via a simple shift $\Delta_2 \equiv \sqrt{2T/W}(1/2T_2)$:

$$\begin{aligned} v_9(f) &= v_8(f) + \Delta_2, & v_{10}(f) &= v_2(f) + \Delta_2, \\ v_{11}(f) &= v_8(f) - \Delta_2, & v_{12}(f) &= v_2(f) - \Delta_2. \end{aligned}$$

The remaining two arguments in equation (A4) are

$$\begin{aligned} v_{13}(f)^2 &= (v_1(f) + \Delta_2)^2 + \frac{2T}{T_2}, \\ v_{14}(f)^2 &= (v_1(f) - \Delta_2)^2 - \frac{2T}{T_2}. \end{aligned}$$

As before, all $w_i(f)$ are determined via $w_i(f) = v_i(-f)$.